Wireless Networks
https://doi.org/10.1007/s11276-023-03366-w

# Joint activity and channel estimation for asynchronous grant-Free NOMA with chaos sequence

Mingyi Qiu[1] · Donghong Cai[1] · Jing Zhao[2] · Zhicheng Dong[3] · Weixi Zhou[4]

Accepted: 13 April 2023


**Abstract**
This paper considers an asynchronous grant-free non-orthogonal multiple access (NOMA) systems which can be applied in massive machine-type communications (mMTCs) and underwater IoT acoustic communication scenarios due to its high spectral efficiency and low power consumption characteristics. In particular, the system's asynchronous reception of user signals can effectively reduce the additional overhead caused by synchronous reception. We investigate the joint activity and channel estimation in the asynchronous case, where an asynchronous frame structure is considered, and a pilot sequence designed by chaotic sequence is used to reduce the pilot storage space. The joint estimations are formulated as single measurement vector (SMV) and multiple measurement vector (MMV) problems for single-antenna and multiple-antenna systems. Different from the existing estimation algorithms, where prior information is considered for estimation, an adaptive alternating direction method of multiplier (ADMM)is proposed for the SMV problem and a two-stage ADMM is proposed for the MMV problem. In particular, an index set is first estimated in each iteration of our proposed adaptive ADMM, and a linear ADMM is performed based on the index set. The first stage of our proposed two-stage ADMM is to estimate the delay and the activity, and then the channel state information is estimated. Further, we analyze the complexity of the two algorithms and their sensitivity to the initial values of chaotic sequences. Finally, simulation results reflecting the detection performance of the algorithms are given. Based on the simulation results, the proposed two algorithms are computationally efficient, providing superior signal recovery accuracy and user activity detection performance. More importantly, the signal delay has a relatively small impact on the proposed algorithm.

**Keywords** Adaptive alternating direction method of multiplier (ADMM) · Asynchronous grant-free NOMA · Chaos sequence · Underwater IoT

## 1 Introduction

With the dramatic growth of IoT devices and wireless network data, future communication technology has higher requirements for spectrum efficiency, energy consumption, response delay and connection in massive machine-type communications (mMTCs) [1, 2]. As the research focus of B5G wireless communication technology, there are always particular technical challenges to realize low-latency reliable communication in mMTC with limited bandwidth

✉ Donghong Cai
dhcai@jnu.edu.cn

✉ Jing Zhao
kettyzj@163.com

Mingyi Qiu
qiumingyihh@163.com

Zhicheng Dong
dongzc666@163.com

Weixi Zhou
zhouweixi@sicnu.edu.cn

[1] College of Information Science and Technology, Jinan University, Guangzhou 510632, China

[2] School of Network and Communication Engineering, Chengdu Technological University, Chengdu 611730, China

[3] School of Information Science and Technology, Tibet University, Lhasa 850000, China

[4] School of Computer Science, Chengdu 695014, China

Published online: 13 June 2023

resources. Especially, underwater communication based on acoustic propagation has stricter requirements for energy efficiency [3, 4]. Generally, to prolong the life of the device, only a few of the devices or users in mMTC are active simultaneously. In this sporadic communication mode, the base station (BS) will find active users according to the data received at different moments. Therefore, detecting active user devices and accurately decoding their data with low latency and low power consumption will be challenging in various communication scenarios, especially for underwater acoustic network communication.

Grant-free access [5, 6] and NOMA [7, 8] are promising solutions to the problems of low-latency communication and massive connection, respectively. As there is no requirement for any verification or authorization, the delay of the signal can be reduced in communication. In NOMA, different users can reuse channel resources to provide more user connections and achieve higher spectrum efficiency. Therefore, NOMA technology is desirable attractive for underwater communication where resources are minimal [9–11]. In [9], NOMA communication is used for multi-user underwater communication, while the MMW-NOMA technique based on a node-pairing algorithm is applied to an underwater acoustic network [10]. Furthermore, [11] is based on NOMA with relay assistance to optimize the power of the devices and maximize the secrecy performance of the underwater communication network.

In [12], the sparsity of the underwater acoustic channel is described. Therefore, the channel estimation and signal detection process in underwater communication can be viewed as a sparse signal recovery problem and solved using a signal estimation algorithm. In the massive IoT, the research on channel estimation, user and data detection has attracted much attention [13–21]. For example, in [13], a two-stage scheme is given, in which the pilot is first sent to detection, and then the data is estimated. In [16], a method based on the EP algorithm is proposed, which is used for the estimation of the signal. AMP algorithm is widely used in signal estimation, and various improved AMP algorithms abound. Initially, the AMP algorithm was used in SMV systems [17]. Then, the improved AMP was applied to MMV systems [18]. In [19] and [20], the author combined the Vector-AMP algorithm [21] with the MMSE denoiser to propose an MMV-AMP method. Besides, [22] adopted a parallel AMP method with improved computational efficiency. However, the above research is based on the premise that different users are fully synchronized. This synchronization scheme does not make sense in practice, since the timing of the signals sent by various users to the base station can vary over time. Therefore, research based on asynchronous scenarios is essential.

Recently, many works have discussed the asynchronous grant-free access system [23–30]. In the asynchronous NOMA scenario in [23], the signal frame is divided into segments, and each segment is processed separately by the AMP algorithm to reduce the complexity. In [26], aiming at the pilot pollution caused by asynchrony, an LMMSE estimator for asynchrony estimation is designed. For the problem of inter-symbol interference caused by asynchronous transmission, [27] designs a pilot with a two-part structure based on the grant-free NOMA system to deal with it; Whereas in [28], a Bayesian receiver composed of two modules is designed for processing, including signal decomposition and time delay estimation. The research [29] considered a blind MIMO detection problem and proposed a Turbo-BiG-AMP algorithm to solve it. In addition, a learnable AMP network is proposed in [30], where parameter learning of the network is performed by model driving.

It should be noted that in the signal processing algorithm mentioned above, most of the pilots used are randomly generated Gaussian matrices, which requires additional storage space for pilots. A chaotic system [31] is a nonlinear system that is uniquely determined by the initial seed and susceptible to the initial value. Therefore, taking the sequence generated by a chaotic map as the pilot matrix only needs to store and transmit the initial seed, saving the space overhead for storing the pilot.

In this paper, based on the scenario of asynchronous grant-free NOMA, we conduct the activity and channel joint estimation in SMV and MMV problems, respectively. We will propose a new estimation scheme based on ADMM, which will be applied to SMV and MMV problems, respectively. Different from the joint estimation algorithms in [32] and [33], it deals with asynchronous issues here. The asynchronous delay is reflected in the pilot design. Here, the Chebyshev chaotic sequence generates the pilot, and gaps of different lengths are added to the pilot to simulate the signal delay. Then, in the SVM scenario, we solve it using a low-complexity linear ADMM algorithm, as discussed in previous work [34]. In addition, with the need for greater accuracy, an adaptive ADMM algorithm framework is proposed based on the index set update. This idea of index set update was first put forward in [35], and later it was applied to many different scenes [36, 37]. A two-stage ADMM approach is proposed for its sparse hierarchical structure to solve the MMV problem. A summary of our contribution is as follows:

- To reduce the storage space of pilot sequences, a chaotic sequence is used to generate a pilot matrix. An adaptive ADMM is proposed for the SMV problem. In particular, an outer loop of index set updating is added outside the adaptive ADMM. The outer circle of the algorithm is used to update the index set, and the inner

loop is used to estimate the signal under the corresponding index set.

- A sparse hierarchical structure of a joint $l_1$-norm and $l_{2,1}$-norm regular equation acting on the MMV problem. A two-stage ADMM is proposed to solve this equation. In the first stage, whether each user is active or not and their signal delay is estimated based on block sparsity. In the second stage, the channel information of each user is accurately estimated.
- Finally, for the proposed method, the main reasons that affect the complexity are analyzed, and the influence of signal delay and SNRs is revealed. Based on the simulation results, the proposed two algorithms are computationally efficient while providing superior signal recovery accuracy and activity detection performance. Moreover, the proposed algorithm has strong stability for the delay.

## 2 System model

Consider an asynchronous frame grant-free uplink NOMA system for the underwater IoT, where the base station (BS) serves $N$ potential active single-antenna users. In order to save energy consumption and extend the life of underwater IoT devices, the potential user is activated sporadically with a small probability and transmits its data to the BS. Therefore, when the signal arrives at the BS, the BS will process it asynchronously for different users. It is assumed that the signals of active users are synchronous at the symbol duration level with some unknown symbol delays. The frame structure of the asynchronous grant-free NOMA system is shown in Fig. 1. In particular, the maximal symbol delay $D$ is not large than the guard time $T_g$, i.e., $D \le T_g$. In this paper, we will set $T_g = D$, and the duration of pilot observation is $L + D$, where the pilot sent by the user is a sequence of length $L$.

Unlike the pilot sequences generated by random sequences, which require considerable storage space, we consider a pilot sequence introduced by Chebyshev chaotic map [31], in which only the initial seeds and main parameters must be stored. Thus the pilot storage space is significantly reduced. Especially, the $l$th $(l = 1, 2 \ldots, L)$ symbol of the pilot sequence for user $n$ $(n = 1, 2, \ldots, N)$ is defined as

$$a_{n,l} = \cos(\tau \cdot \arccos(a_{n,l-1})), \tag{1}$$

where $a_{n,0} \in [-1, 1]$ is the initial seed for user $n$. Then the unique normalized $L(L \ll N)$-length sequence $\mathbf{a}_n = \left(a_{n,1}, a_{n,2}, \ldots a_{n,L}\right)^T \in \mathbb{R}^{L\times 1}$ for the $n$th user is obtained by normalizing $L$ outputs of the Chebyshev map defined in (1) with seed $a_{n,0}$. It is essential to point out that each user only needs to protect its own initial seed from enhancing the security of the pilot sequence. Besides, the real sequence defined in (1) can be easily extended to the complex sequence by producing the imaginary part with another seed.

For a complete synchronization case, i.e., $D = 0$, the single measurement vector (SMV) signal is received by the BS with a single-antenna as indicated below

$$\begin{aligned}\tilde{\mathbf{y}} &= [\mathbf{a}_1, \mathbf{a}_2, \ldots, \boldsymbol{a}_N](\omega_1 h_1, \omega_2 h_2, \ldots, \omega_N h_N)^T + \tilde{\mathbf{w}} \\ &= \mathbf{A}\boldsymbol{\Omega}\boldsymbol{h} + \tilde{\mathbf{w}} \\ &\triangleq \mathbf{A}\tilde{\mathbf{e}} + \tilde{\mathbf{w}},\end{aligned} \tag{2}$$

where $\mathbf{A} = [\mathbf{a}_1, \mathbf{a}_2, \ldots, \mathbf{a}_N] \in \mathbb{R}^{L\times N}$ is the pilot matrix, $\boldsymbol{\Omega} = \mathbf{diag}(\boldsymbol{\omega})$ with $\boldsymbol{\omega} = (\omega_1, \omega_2, \ldots, \omega_N)$ is an indicator matrix for all users to be active or not. In particular, $\omega_n = 1$ denotes the active state of user $n$, and $\omega_n = 0$ means the inactive state. Besides, $\mathbf{h} = (h_1, h_2, \ldots, h_N)^T$ denotes the channel coefficient vector associated with all users. $\tilde{\mathbf{w}} \sim \mathcal{N}_c(\mathbf{0}, \sigma_{\tilde{\mathbf{w}}}^2 \mathbf{I}_L)$ is an additive white Gaussian noise (AWGN) vector.

For the asynchronous case, i.e., $D \ge 1$, the pilot sequence $\mathbf{a}_n$ of user $n$ can be expanded to an $\tilde{L} \times (t_n + 1)$ matrix $\mathbf{A}_n = [\tilde{\mathbf{a}}_{n1}, \tilde{\mathbf{a}}_{n2}, \ldots, \tilde{\mathbf{a}}_{n(t_n+1)}]$ representing all possible measurements within delay $t_n (t_n \le D)$, where $\tilde{\mathbf{a}}_{nj} = \left(\tilde{a}_{nj,1}, \ldots, \tilde{a}_{nj,t_n+1}, \ldots, \tilde{a}_{nj,\tilde{L}}\right)^T \in \mathbb{R}^{\tilde{L}\times 1}$ is the $j$th possible measurement of pilot sequence, and $\tilde{L} = L + t_n, j = 1, 2 \ldots, t_n + 1$. In particular, $\tilde{\mathbf{a}}_n$ is obtained by inserting $t_n$ zeros before $\mathbf{a}_n$ and $D - t_n$ zeros after $\mathbf{a}_n$, i.e., $\tilde{\mathbf{a}}_n = \left(\mathbf{0}_{t_n}^T, \mathbf{a}_n^T, \mathbf{0}_{D-t_n}^T\right)^T$. Moreover, $\boldsymbol{\Omega}_n = \mathbf{diag}(\boldsymbol{\omega}_n) \in \mathbb{R}^{(D+1)\times(D+1)}$ with $\boldsymbol{\omega}_n = (\omega_{n1}, \omega_{n2}, \ldots, \omega_{n(D+1)})^T$ denotes the equivalent activity, where only one element of $\boldsymbol{\omega}_n$ is one, and other elements are zeros. Then the SMV can be formulated as

$$\begin{aligned}\mathbf{y} &= \tilde{\mathbf{A}}\tilde{\boldsymbol{\Omega}}\tilde{\mathbf{h}} + \mathbf{w} \\ &\triangleq \tilde{\mathbf{A}}\mathbf{e} + \mathbf{w},\end{aligned} \tag{3}$$

in which matrix $\tilde{\mathbf{A}} = [\mathbf{A}_1, \mathbf{A}_2, \ldots, \mathbf{A}_N] \in \mathbb{C}^{\tilde{L}\times N(D+1)}$ collects the pilot of all users, $\tilde{\boldsymbol{\Omega}} = \mathbf{diag}(\boldsymbol{\Omega}_1, \boldsymbol{\Omega}_2, \ldots, \boldsymbol{\Omega}_N) \in \mathbb{C}^{N(D+1)\times N(D+1)}$, $\tilde{\mathbf{h}} = ((\mathbf{1}_{D+1} h_1)^H, \ldots, (\mathbf{1}_{D+1} h_N)^H)^H \in \mathbb{C}^{N(D+1)}$, and $\mathbf{w} \in \mathbb{C}^{\tilde{L}\times 1}$ is the AWGN vector.

Furthermore, the multiple measurement vectors (MMVs) problem for the BS with $M$ antennas is

$$\mathbf{Y} = \tilde{\mathbf{A}}\tilde{\boldsymbol{\Omega}}\mathbf{H} + \mathbf{W} \triangleq \tilde{\mathbf{A}}\mathbf{E} + \mathbf{W}, \tag{4}$$

where $\mathbf{H} = [\tilde{\mathbf{h}}_1, \tilde{\mathbf{h}}_2, \ldots, \tilde{\mathbf{h}}_M] \in \mathbb{C}^{N(D+1)\times M}$ denotes the channel matrix, and $\mathbf{E} = \tilde{\boldsymbol{\Omega}}\mathbf{H} \in \mathbb{C}^{N(D+1)\times M}$ is the effective channel matrix, and $\mathbf{W} \in \mathbb{C}^{\tilde{L}\times M}$ is an AWGN matrix.

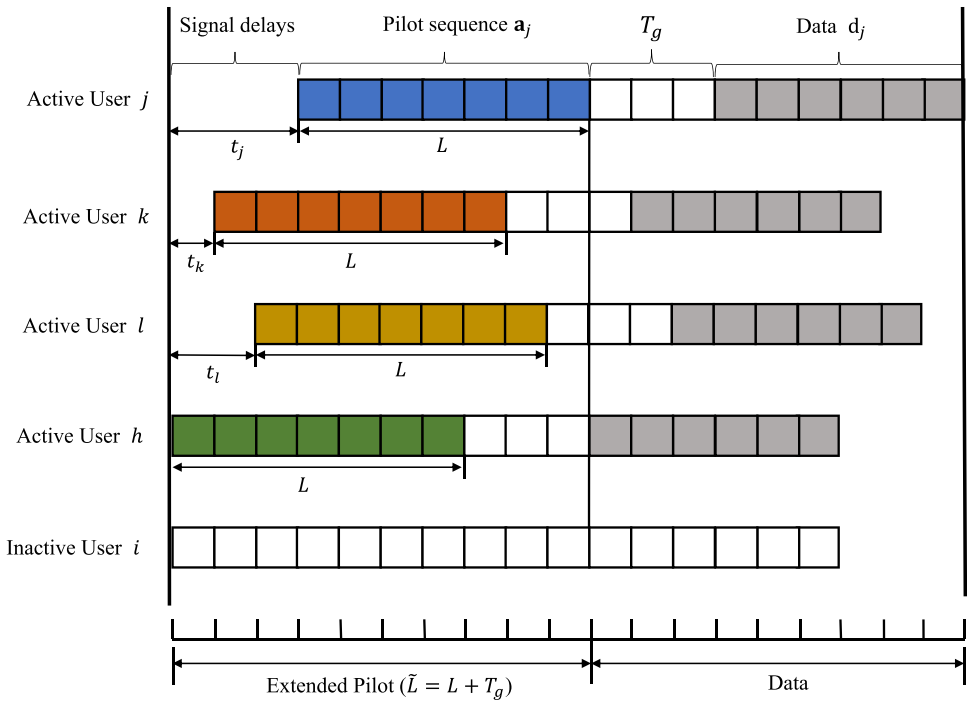


**Fig. 1** The frame structure of asynchronous grant-free NOMA system

Note that the SMV and MMV problems formulated in (3) and (4) are both sparse recovery problems due to the sporadic activity of users. Different from the existing works, where some prior information or Gaussian measurement matrix is required, the aim of this paper is to chaotic sparse measurement problems without any prior information.

## 3 Proposed adaptive ADMM algorithm for SMV problem

We propose an adaptive ADMM algorithm for the activity and channel joint estimation of asynchronous grant-free uplink NOMA in this section. In particular, the joint estimation is first formulated as an SMV problem, which is a sparse recovery problem. Unlike the ADMM algorithm, where all of the elements of the sparse vector are estimated in each iteration. The proposed adaptive ADMM algorithm selects part of elements with small amplitudes to perform low-complexity ADMM estimation in each iteration of the outer loop. To this end, a sparse recovery framework based on the index set update is introduced for the outer loop and a linear ADMM is derived for the inner loop.

The joint estimation for the SMV in (3) is formulated as

$$\min_{\mathbf{e}\in\mathbb{C}^{N(D+1)}} \|\mathbf{e}\|_0 \tag{5a}$$

$$\text{s.t. } \|\mathbf{y} - \tilde{\mathbf{A}}\mathbf{e}\|_2^2 \le \epsilon, \tag{5b}$$

where parameter $\epsilon > 0$ is determined by Gaussian noise. It is challenging to handle the problem (5) which is an NP-hard problem. Consequently, problem (5) is further related as

$$\min_{\mathbf{e}\in\mathbb{C}^{N(D+1)}} \|\mathbf{e}\|_1 \tag{6a}$$

$$\text{s.t. } \|\mathbf{y} - \tilde{\mathbf{A}}\mathbf{e}\|_2^2 \le \epsilon. \tag{6b}$$

Note that all of the elements in sparse vector $\mathbf{e}$ can be estimated by solving the optimization problem (6). However, the estimation accuracy is difficult to guarantee because most elements are zeros. Especially, the performance of activity detection will degrade significantly without perfect prior information or an appropriate threshold. To this end, the $k$th estimation of $\mathbf{e}$ based on the problem (6)

$$\mathbf{e}^{(k)} = \operatorname*{argmin}_{\mathbf{e}\in\mathbb{C}^{N(D+1)}} \|\mathbf{e}\|_{\Upsilon^{(k)},1} \tag{7a}$$

$$\text{s.t. } \|\mathbf{y} - \tilde{\mathbf{A}}\mathbf{e}\|_2^2 \le \epsilon, \tag{7b}$$

where the set $\Upsilon^{(k)}$ is obtained by

$$\Upsilon^{(k)} = \{i : |e_i^{(k-1)}| \le \varpi^{(k-1)}\} \tag{8}$$

with threshold $\varpi^{(k)} = \|\mathbf{e}^{(k)}\|_\infty / \beta^{k-1}$, $\beta^{k-1} \ge 1$ is parameter, and $\|\mathbf{e}\|_{\Upsilon^{(k)},1} = \sum_{i\in\Upsilon^{(k)}} |e_i^{(k)}|$. Different from (6), problem (7) is solved according to the set $\Upsilon^{(k)}$. It is important to point out that the set $\Upsilon^{(k)}$ is the index set of elements with a smaller amplitude in $\mathbf{e}^{(k)}$. The aim of the problem (7) is to find the solution under constraint (7b) such that the sum of

the amplitudes of elements over set $\Upsilon^{(k)}$ is minimal. The proposed sparse recovery framework based on iterative index update is summarized (Fig. 2):

- Step 1: The set $\Upsilon^{(k)}$ is updated in (8).
- Step 2: The sparse signal vector $\mathbf{e}^{(k)}$ is obtained by solving problem (7).
- Step 3: The threshold $\varpi^{(k)}$ in set $\Upsilon^{(k)}$ is updated.

To solve the problem (7) effectively, a linear ADMM algorithm is proposed. The corresponding unconstrained optimization problem for the problem (7) is formulated as

$$\min_{\mathbf{e}\in\mathbb{C}^{N(D+1)}} \frac{1}{2}\|\mathbf{y}-\tilde{\mathbf{A}}\mathbf{e}\|_2^2+\gamma\|\mathbf{e}\|_{\Upsilon^{(k)},1}, \tag{9}$$

where the regularization parameter $\gamma \geq 0$. Adding the variable $\mathbf{z}$ simplifies the solution of (9) as

$$\min_{\mathbf{e}\in\mathbb{C}^{N(D+1)}} \frac{1}{2}\|\mathbf{y}-\tilde{\mathbf{A}}\mathbf{e}\|_2^2+\gamma\|\mathbf{z}\|_{\Upsilon^{(k)},1} \tag{10a}$$

$$\text{s.t. } \mathbf{e}=\mathbf{z}, \tag{10b}$$

Consequently, we can obtain the augmented Lagrange function of (10)

$$\mathcal{L}(\mathbf{e},\mathbf{z},\mathbf{u})=\frac{1}{2}\|\mathbf{y}-\tilde{\mathbf{A}}\mathbf{e}\|_2^2+\gamma\|\mathbf{z}\|_{\Upsilon^{(k)},1}+\frac{\rho}{2}\|\mathbf{e}-\mathbf{z}+\mathbf{u}\|_2^2, \tag{11}$$

where the constant parameter $\rho > 0$, and the variable $\mathbf{u}$ is the multiplier of (11), also called a dual variable. Subsequently, we can then decompose (11) into several subproblems to be solved, with the $t$th iteration proceeding as

$$\mathbf{e}^{(t+1)}=\underset{\mathbf{e}\in\mathbb{C}^{N(D+1)}}{\operatorname{argmin}} \frac{1}{2}\|\mathbf{y}-\tilde{\mathbf{A}}\mathbf{e}\|_2^2+\frac{\rho}{2}\|\mathbf{e}-\mathbf{z}^{(t)}+\mathbf{u}^{(t)}\|_2^2, \tag{12a}$$

$$\mathbf{z}^{(t+1)}=\underset{\mathbf{z}\in\mathbb{C}^{N(D+1)}}{\operatorname{argmin}} \gamma\|\mathbf{z}\|_{\Upsilon^{(k)},1}+\frac{\rho}{2}\|\mathbf{z}-\mathbf{e}^{(t+1)}-\mathbf{u}^{(t)}\|_2^2, \tag{12b}$$

$$\mathbf{u}^{(t+1)}=\mathbf{u}^{(t)}+\mathbf{e}^{(t+1)}-\mathbf{z}^{(t+1)}, \tag{12c}$$

Firstly, the (12a) is convex and differentiable to the variable $\mathbf{e}$. Take the derivative of (12a), and we can get

$$(\tilde{\mathbf{A}}\mathbf{e}-\mathbf{y})^H\tilde{\mathbf{A}}+\rho(\mathbf{e}-\mathbf{z}^{(t)}+\mathbf{u}^{(t)})^H=\mathbf{0}, \tag{13}$$

After a simple calculation we obtain

$$\mathbf{e}^{(t+1)}=(\rho\mathbf{I}_N+\tilde{\mathbf{A}}^H\tilde{\mathbf{A}})^{-1}\left(\tilde{\mathbf{A}}^H\mathbf{y}+\rho(\mathbf{z}^{(t)}-\mathbf{u}^{(t)})\right). \tag{14}$$

In (14), we can see that its primary computational consumption lies in the multiplication and inversion of the matrix. As we know, an increase in users and the asynchronous signal delay will bring an increase in the size of matrix $\tilde{\mathbf{A}}$, which in turn leads to a dramatic increase in complexity. Considering the efficiency of solving the algorithm and avoiding the inverse operation of the matrix, we can treat (12a) as

$$\mathbf{e}^{(t+1)}=\underset{\mathbf{e}\in\mathbb{C}^{N(D+1)}}{\operatorname{argmin}} \frac{1}{2}\|\bar{\mathbf{A}}\mathbf{e}-\bar{\mathbf{y}}\|_2^2, \tag{15}$$

where the matrix $\bar{\mathbf{A}}=(\tilde{\mathbf{A}}^H,\sqrt{\rho}\mathbf{I}_N)^H$ and $\bar{\mathbf{y}}=(\mathbf{y}^H,\sqrt{\rho}(\mathbf{z}^{(t)}-\mathbf{u}^{(t)})^H)^H$.

Let $f(\mathbf{e})=\frac{1}{2}\|\bar{\mathbf{A}}\mathbf{e}-\bar{\mathbf{y}}\|_2^2$ denote the objective function of (15), then perform a Taylor expansion at $\mathbf{e}^{(t)}$,

$$\begin{aligned} f(\mathbf{e}) &= f(\mathbf{e}^{(t)})+\mathrm{Re}[\nabla f(\mathbf{e}^{(t)})(\mathbf{e}-\mathbf{e}^{(t)})] \\ &\quad+\frac{1}{2}(\mathbf{e}-\mathbf{e}^{(t)})^H\nabla^2 f(\mathbf{e}^{(t)})(\mathbf{e}-\mathbf{e}^{(t)}) \\ &\approx f(\mathbf{e}^{(t)})+\mathrm{Re}[\nabla f(\mathbf{e}^{(t)})(\mathbf{e}-\mathbf{e}^{(t)})]+\frac{\mu^{(t)}}{2}\|\mathbf{e}-\mathbf{e}^{(t)}\|_2^2, \end{aligned} \tag{16}$$

where the parameter $\mu^{(t)} > 0$ is used for the approximation of the second-order derivative $\nabla^2 f(\mathbf{e}^{(t)})$, and $\mu^{(t)}$ is dynamically adjusted with the result of each iteration, defined as

$$\mu^{(t)}=\frac{\|\tilde{\mathbf{A}}(\mathbf{e}^{(t)}-\mathbf{z}^{(t)})\|_2^2}{\|(\mathbf{e}^{(t)})-\mathbf{z}^{(t)}\|_2^2}. \tag{17}$$

We submit (16) into (15) and can obtain

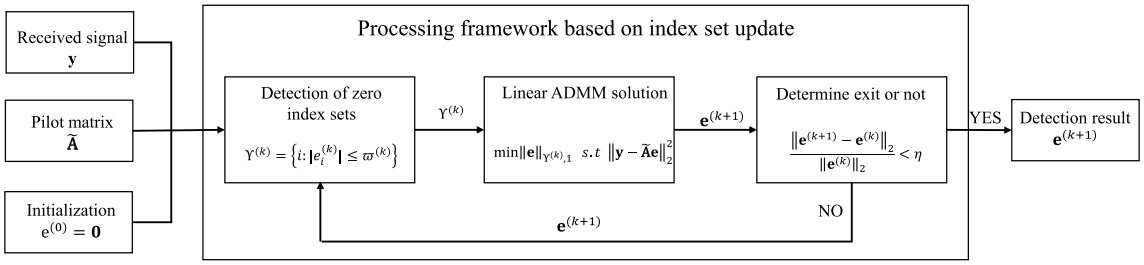


**Fig. 2** Proposed adaptive ADMM framework

$$\begin{aligned}\mathbf{e}^{(t+1)} &= \underset{\mathbf{e}\in\mathbb{C}^{N(D+1)}}{\operatorname{argmin}} \frac{\mu^{(t)}}{2}\left(2\mathrm{Re}\left[\frac{1}{\mu^{(t)}}\nabla f(\mathbf{e}^{(t)})(\mathbf{e}-\mathbf{e}^{(t)})\right]+\|\mathbf{e}-\mathbf{e}^{(t)}\|_2^2\right)\\ &= \underset{\mathbf{e}\in\mathbb{C}^{N(D+1)}}{\operatorname{argmin}} \frac{\mu^{(t)}}{2}\|\mathbf{e}-\mathbf{e}^{(t)}+\frac{1}{\mu^{(t)}}\nabla f(\mathbf{e}^{(t)})\|_2^2.\end{aligned} \tag{18}$$

Accordingly, the $t$th update of (12a)is

$$\begin{aligned}\mathbf{e}^{(t+1)} &= \mathbf{e}^{(t)}-\frac{1}{\mu^{(t)}}\nabla f(\mathbf{e}^{(t)})\\ &= \mathbf{e}^{(t)}-\frac{1}{\mu^{(t)}}\bar{\mathbf{A}}^H(\bar{\mathbf{A}}\mathbf{e}^{(t)}-\bar{\mathbf{y}}).\end{aligned} \tag{19}$$

For sub-problem (12b), the elements of solution over index set $\Upsilon^{(k)}$ is obtained by

$$\begin{aligned}\mathbf{z}_{\Upsilon^{(k)}}^{(t+1)} &= \underset{\mathbf{z}\in\mathbb{C}^{N(D+1)}}{\operatorname{argmin}} \gamma\|\mathbf{z}\|_{\Upsilon^{(k)},1}+\frac{\rho}{2}\|\mathbf{z}_{\Upsilon^{(k)}}-\mathbf{e}_{\Upsilon^{(k)}}^{(t+1)}-\mathbf{u}_{\Upsilon^{(k)}}^{(t)}\|_2^2\\ &= \mathrm{shrink}_1\left(\mathbf{e}_{\Upsilon^{(k)}}^{(t+1)}+\mathbf{u}_{\Upsilon^{(k)}}^{(t+1)},\frac{\gamma}{\rho}\right),\end{aligned} \tag{20}$$

The threshold function $\mathrm{shrink}_1$ is consistent with the definition in [38]. The elements of the solution $\mathbf{z}^{(k+1)}$ over the complement of the index set $\Upsilon^{(k)}$ is

$$\mathbf{z}_{(\Upsilon^{(k)})^C}^{(t+1)} = \mathbf{e}_{(\Upsilon^{(k)})^C}^{(t+1)}+\mathbf{u}_{(\Upsilon^{(k)})^C}^{(t)}. \tag{21}$$

The solution $\mathbf{z}^{(t+1)}$ of sub-problem (12b) is then obtained based on (20) and (21).

Therefore, the updates of (17), (19), (20), and (21) are repeated until the exit condition is satisfied:

$$\frac{\|\mathbf{e}^{(t+1)}-\mathbf{e}^{(t)}\|_2}{\|\mathbf{e}^{(t+1)}\|_2}<\eta, \tag{22}$$

where $\eta>0$ is a constant, which is specified according to the precision required. Finally, in Algorithm 1 we can see the overall process of the proposed algorithm.

**Algorithm 1** Proposed Adaptive ADMM for SMV Problem

**Input:** $\tilde{\mathbf{A}}, \mathbf{y}$.
**Output:** $\hat{\mathbf{e}}$.
**Outer-Loop Initialization:** $\mathbf{e}^{(0)}=\mathbf{0}, \varpi^{(0)}=1, \beta, \gamma, \rho, \eta$.

**for** $k=1,2,\cdots,k_{max}$ **do**
  $\mathbf{e}_{old}=\mathbf{e}^{(k-1)}$;
  $\Upsilon^{(k)}=\{i:|e_i^{(k-1)}|\le\varpi^{(k-1)}\}$;
  **Inner-Loop: Solving problem** (7)
  **for** $t=1,2,\cdots,t_{max}$ **do**
    $\mu^{(t)}=\frac{\|\bar{\mathbf{A}}(\mathbf{e}^{(t)}-\mathbf{z}^{(t)})\|_2^2}{\|\mathbf{e}^{(t)}-\mathbf{z}^{(t)}\|_2^2}$;
    $\mathbf{e}^{(t+1)}=\mathbf{e}^{(t)}-\frac{1}{\mu}\bar{\mathbf{A}}^T(\bar{\mathbf{A}}\mathbf{e}^{(t)}-\bar{\mathbf{y}})$;
    $\mathbf{z}_{\Upsilon^{(k)}}^{(t+1)}=\mathrm{shrink}_1\left(\mathbf{e}_{\Upsilon^{(k)}}^{(t+1)}+\mathbf{u}_{\Upsilon^{(k)}}^{(t+1)},\frac{\gamma}{\rho}\right)$;
    $\mathbf{z}_{(\Upsilon^{(k)})^C}^{(t+1)}=\mathbf{e}_{(\Upsilon^{(k)})^C}^{(t+1)}+\mathbf{u}_{(\Upsilon^{(k)})^C}^{(t+1)}$;
    $\mathbf{u}^{(t+1)}=\mathbf{u}^{(t)}+\mathbf{e}^{(t+1)}-\mathbf{z}^{(t+1)}$;
    **if** $\frac{\|\mathbf{e}^{(t+1)}-\mathbf{e}^{(t)}\|_2}{\|\mathbf{e}^{(t+1)}\|_2}<\eta$ **then**
      break;
    **end if**
  **end for**
  $\mathbf{e}^{(k)}\leftarrow$ From loop 5 to 14.
  $\varpi^{(k)}=\|\mathbf{e}^{(k)}\|_\infty/\beta^{k-1}$;
  **if** $\frac{\|\mathbf{e}^{(k)}-\mathbf{e}_{old}\|_2}{\|\mathbf{e}^{(k)}\|_2}<\eta$ **then**
    break;
  **end if**
**end for**
**Return:** $\hat{\mathbf{e}}$.

## 4 Proposed two-stage-ADMM for MMV problem

Different to the SMV problem, the sparse recovery for MMV problem (4) with multiple-antenna BS is expressed as

$$\min_{\mathrm{vec}(\mathbf{E})} \|\mathrm{vec}(\mathbf{E})\|_0 \tag{23a}$$

$$\text{s.t. } \|\mathrm{vec}(\mathbf{Y}) - (\mathbf{I}_M \otimes \tilde{\mathbf{A}})\mathrm{vec}(\mathbf{E})\|_2^2 \le \epsilon, \tag{23b}$$

where the operation of converting a matrix into a vector is $\mathrm{vec}(\cdot)$.

Similarly, we can relax the problem (23) and deal with it by joint norm

$$\min_{\mathbf{E}} \frac{1}{2}\|\mathbf{Y} - \tilde{\mathbf{A}}\mathbf{E}\|_F^2 + \gamma_1\|\mathbf{E}\|_1 + \gamma_2\|\mathbf{E}\|_{2,1}, \tag{24}$$

The regular parameters $\gamma_1 \ge 0, \gamma_2 \ge 0$. In (24), the matrix $\mathbf{E}$ is row sparse. Thus, the $l_1$-norm is used to constrain the overall sparsity, while the $l_{2,1}$-norm is used to constrain the row sparsity.

Under the joint norm constraint, we can still use the idea of linear ADMM to solve (24). However, the straightforward solution has high complexity and low precision. Therefore, we consider (24) as a two-part process to meet efficiency and accuracy requirements and propose a two-stage ADMM algorithm.

In the first stage, considering the effect of signal delay $T_g = D$, the related channel information of each user is changed from one row of matrix $\mathbf{E}$ to $T_g + 1$ rows. This way, we can transform the sparse constraint on each row in $l_{2,1}$-norm term into the constraint on $T_g + 1$ rows. The new norm term is denoted as $\sum_{i=1}^{N}\|(\mathbf{E})_i\|_F$, where $(\mathbf{E})_i \in \mathbb{C}^{(T_g+1)\times M}$ is all possible channel information belonging to the $i$th user. Of all these possibilities, only one row is the actual channel coefficient of the user, i.e., only one row is non-zero. Therefore, the first stage of the algorithm is to solve a block sparse constraint problem

$$\min_{\mathbf{E}} \frac{1}{2}\|\mathbf{Y} - \tilde{\mathbf{A}}\mathbf{E}\|_F^2 + \gamma_1 \sum_{i=1}^{N}\|(\mathbf{E})_i\|_F. \tag{25}$$

Furthermore, the augmented Lagrange function of (25) is

$$\begin{aligned}\mathcal{L}(\mathbf{E},\mathbf{Z},\mathbf{U}) = &\frac{1}{2}\|\mathbf{Y} - \tilde{\mathbf{A}}\mathbf{E}\|_F^2 + \gamma_1 \sum_{i=1}^{N}\|(\mathbf{Z})_i\|_F \\ &+ \frac{\rho_1}{2}\|\mathbf{E} - \mathbf{Z} + \mathbf{U}\|_F^2.\end{aligned} \tag{26}$$

Based on the classical ADMM and the idea of (12a), the solution process of (26) is as follows,

(1) Update $\mathbf{E}^{(k+1)}$ as

$$\begin{aligned}\mathbf{E}^{(k+1)} = \mathbf{E}^{(k)} - \frac{1}{\mu_1^{(k)}}\Big(&(\tilde{\mathbf{A}}^H\tilde{\mathbf{A}} + \rho_1\mathbf{I}_N)\mathbf{E}^{(k)} \\ &-\tilde{\mathbf{A}}^H\mathbf{Y} - \rho_1\Big(\mathbf{Z}^{(k)} - \mathbf{U}^{(k)}\Big)\Big)\end{aligned} \tag{27}$$

(2) Update $\mathbf{Z}^{(k+1)}$ as

$$(\mathbf{Z})_i^{(k+1)} = \mathrm{shrink}_{F,1}\left((\mathbf{E})_i^{(k+1)} + (\mathbf{U})_i^{(k)}, \frac{\gamma_1}{\rho_1}\right). \tag{28}$$

where $i = 1, 2, ..., N$.

(3) Update $\mathbf{U}^{(k+1)}$ as

$$\mathbf{U}^{(k+1)} = \mathbf{U}^{(k)} + \mathbf{E}^{(k+1)} - \mathbf{Z}^{(k+1)}. \tag{29}$$

***Remark 1*** By solving (25), we can obtain a block-sparse solution that defines the index set corresponding to a non-zero block as $\mathrm{ind}_1$, i.e., $\mathrm{ind}_1 = \{i|\|(\mathbf{E})_i\|_F \ne 0, i = 1, 2, ..., N\}$.

***Remark 2*** For each non-zero block in $\mathrm{ind}_1$, only one row is channel information belonging to an actual active user.

To find the real location of active users, we take the row with the largest $l_2$-norm in the $i$th non-zero block $(\mathbf{E})_i$ as the estimated active user location and record it as $\mathrm{ind}_2$. Where

$$\mathrm{ind}_2 = \{j|\max(\|(\mathbf{E})_{i,j}\|_2), i = 1, 2, ..., N, j = 1, 2, ..., T_g + 1\},$$

$j$ denotes the $j$th row of $(\mathbf{E})_i$.

In the second stage, we use $l_1$-norm constraint to estimate only the channel coefficients on the index set $\mathrm{ind}_2$.

$$\min_{\mathbf{E}_{\mathrm{ind}_2}} \frac{1}{2}\|\mathbf{Y} - \tilde{\mathbf{A}}_{\mathrm{ind}_2}\mathbf{E}_{\mathrm{ind}_2}\|_F^2 + \gamma_2\|\mathbf{E}_{\mathrm{ind}_2}\|_1. \tag{30}$$

Similarly, the augmented Lagrange function of formula (30) is

$$\begin{aligned}\mathcal{L}(\mathbf{E}_{\mathrm{ind}_2},\mathbf{Z}_{\mathrm{ind}_2},\mathbf{U}_{\mathrm{ind}_2}) = &\frac{1}{2}\|\mathbf{Y} - \tilde{\mathbf{A}}_{\mathrm{ind}_2}\mathbf{E}_{\mathrm{ind}_2}\|_F^2 + \gamma_2\|\mathbf{Z}_{\mathrm{ind}_2}\|_1 \\ &+ \frac{\rho_2}{2}\|\mathbf{E}_{\mathrm{ind}_2} - \mathbf{Z}_{\mathrm{ind}_2} + \mathbf{U}_{\mathrm{ind}_2}\|_F.\end{aligned} \tag{31}$$

Similar to the first stage solution, the process of solving (31) is

(1) Update $\mathbf{E}_{\mathrm{ind}_2}^{(k+1)}$ as

$$\begin{aligned}\mathbf{E}_{\mathrm{ind}_2}^{(k+1)} = &\mathbf{E}_{\mathrm{ind}_2}^{(k)} - \frac{1}{\mu_2^{(k)}}\Big(\Big(\tilde{\mathbf{A}}_{\mathrm{ind}_2}^H\tilde{\mathbf{A}}_{\mathrm{ind}_2} + \rho_2\mathbf{I}_N\Big)\mathbf{E}_{\mathrm{ind}_2}^{(k)} \\ &- \tilde{\mathbf{A}}_{\mathrm{ind}_2}^H\mathbf{Y} - \rho_2\Big(\mathbf{Z}_{\mathrm{ind}_2}^{(k)} - \mathbf{U}_{\mathrm{ind}_2}^{(k)}\Big)\Big).\end{aligned} \tag{32}$$

(2) Update $\mathbf{Z}_{\mathrm{ind}_2}^{(k+1)}$ as

$$\mathbf{z}_i^{(k+1)} = \text{shrink}_1\left(\mathbf{e}_i^{(k+1)} + \mathbf{u}_i^{(k)}, \frac{\gamma_2}{\rho_2}\right). \tag{33}$$

where $\mathbf{z}_i$ is the $i$th column of matrix $\mathbf{Z}_{\text{ind}_2}$, $i = 1, 2, ..., M,$.

(3) Update $\mathbf{U}_{\text{ind}_2}^{(k+1)}$ as

$$\mathbf{U}_{\text{ind}_2}^{(k+1)} = \mathbf{U}_{\text{ind}_2}^{(k)} + \mathbf{E}_{\text{ind}_2}^{(k+1)} - \mathbf{Z}_{\text{ind}_2}^{(k+1)}. \tag{34}$$

Similar to (22), the condition for loop exit is

$$\frac{\|\mathbf{E}^{(k+1)} - \mathbf{E}^{(k)}\|_2}{\|\mathbf{E}^{(k+1)}\|_2} < \eta. \tag{35}$$

The proposed two-stage ADMM algorithm is summarized in Algorithm 2.

improves computational efficiency and estimation accuracy.

## 5 Complexity analysis

This section will analyze the steps within the algorithm that contribute the most to the complexity.

As can be obtained in Algorithm 1, the primary computational consumption in the loop comes from the multiplication calculation of Eq. (19). In this step, a total of $\mathbb{K}(\mathbb{T}_0(3N(T_g+1)+2\tilde{L}N(T_g+1)))$ multiplication operations are performed, where $\mathbb{K}$ and $\mathbb{T}_0$ represent the times of the outer loop and inner loop, respectively.

Similarly, (27) and (32) are the primary computational costs of algorithm 2 in two stages, respectively. In the first

**Algorithm 2** Proposed Two-Stage-ADMM for MMV Problem

**Input:** $\tilde{\mathbf{A}}, \mathbf{Y}$.
**Output:** $\hat{\mathbf{E}}$.
**Initialization:** $\mathbf{E}^{(0)}, \mathbf{Z}^{(0)}, \mathbf{U}^{(0)}, \gamma_1, \rho_1, \gamma_2, \rho_2, \eta$.
**Loop in stage 1:**

**for** $k = 1, 2, \cdots, k_{max}$ **do**
  $\mu_1^{(k)} = \frac{\|\tilde{\mathbf{A}}(\mathbf{E}^{(k)} - \mathbf{Z}^{(k)})\|_F^2}{\|(\mathbf{E}^{(k)}) - \mathbf{Z}^{(k)}\|_F^2}$;
  Update $\mathbf{E}^{(k+1)}$ by using (27);
  Update $\mathbf{Z}^{(k+1)}$ by using (28);
  Update $\mathbf{U}^{(k+1)}$ by using (29);
  **if** (35) **then**
    break;
  **end if**
**end for**

**Return the support set** $\text{ind}_2$
**Loop in stage 2:**

**for** $k = 1, 2, \cdots, k_{max}$ **do**
  $\mu_2^{(k)} = \frac{\|\tilde{\mathbf{A}}_{\text{ind}_2}(\mathbf{E}_{\text{ind}_2}^{(k)} - \mathbf{Z}_{\text{ind}_2}^{(k)})\|_F^2}{\|(\mathbf{E}_{\text{ind}_2}^{(k)}) - \mathbf{Z}_{\text{ind}_2}^{(k)}\|_F^2}$;
  Update $\mathbf{E}_{\text{ind}_2}^{(k+1)}$ by using (32);
  Update $\mathbf{Z}_{\text{ind}_2}^{(k+1)}$ by using (33);
  Update $\mathbf{U}_{\text{ind}_2}^{(k+1)}$ by using (34);
  **if** (35) **then**
    break;
  **end if**
**end for**

**Return:** $\hat{\mathbf{E}}$.

***Remark 3*** We transformed (24) into a two-stage solution, with the first stage considering only the estimation of active users without specific accuracy and the second stage solving exactly for each user's channel information. This

stage, (27) performed $\mathbb{K}_1(2MN(T_g+1)(\tilde{L}+1))$ times of multiplication. In the second stage, (32) was multiplied $\mathbb{K}_2(2|\text{ind}_2|M(\tilde{L}+1))$ times where $\mathbb{K}_1$ and $\mathbb{K}_2$ are the iteration times in each of the two stages.

## 6 Simulation

We will perform simulation experiments and performance analysis of the linear ADMM algorithm, the adaptive ADMM algorithm, and the two-stage ADMM algorithm. The parameters are set: $N = 256$, the probability of users being active $p = 0.1$, $L = 128$. In particular, the initial seed of the chaotic sequence used to generate the pilot for each user is a random number $a_{n,0} \in [-1, 1], n = 1, 2, ..., N$. In the asynchronous case, the number of users is extended to $N(T_g + 1)$ and $\tilde{L} = L + T_g$.

The performance evaluation of the algorithms for channel estimation is defined as

$$\text{NMSE} = \frac{\|\hat{\Theta} - \Theta\|_2}{\|\Theta\|_2}, \tag{36}$$

where $\Theta = \mathbf{e}$ or $\Theta = \mathbf{E}$. The parameters used to evaluate the performance for active user detection are the false alarm rate (PFA) and the missed detection rate (PMD), defined in [39]. To better describe the PFA and PMD in the simulation results, the same strategy as in [39] is adopted here, where the threshold is set for determining whether it is active. When the estimated value exceeds the threshoud, it is considered active.

In the SMV problem, the parameters of the relevant algorithm are set as: $\beta = 5$, $\gamma = 0.03$, $\eta = 0.0001$, $\rho = 0.1$, and threshold $\in [0, 1]$. A performance comparison of the algorithms is given in Figs. 3 and 4. A NMSE comparison of the linear ADMM, the adaptive ADMM and the AMP is given in Fig. 3, where the signal delays are set as $T_g = 3$ and $T_g = 5$, respectively. We can see that both the linear ADMM algorithm and the AMP algorithm have a decrease in estimation accuracy when the signal delay $T_g$ increases. The linear ADMM algorithm performs better at high SNRs (SNR $\geq$ 25 dB), while the AMP algorithm has an advantage at low SNRs. In addition, the adaptive ADMM algorithm is very accurate, achieving a 5 dB performance improvement at high SNRs. This is attributed to the fact that the usual linear ADMM is deficient in estimating small amplitude signals. In contrast, the adaptive ADMM algorithm only estimates small amplitude signals in each inner loop.

In Fig. 4, the active user detection performance of the algorithm is given for SNR = 25 dB and different signal delays $T_g$. We can observe a significant improvement in PFA and PMD performance for the adaptive ADMM algorithm. In particular, the PFA and PMD performance of the linear ADMM is worse than the AMP at $T_g = 1$. As $T_g$ increases, the performance of linear ADMM is gradually superior to the AMP algorithm. Therefore, it can be concluded that the impact of signal delay $T_g$ on the linear ADMM is less than that of the AMP.

Furthermore, we consider the MMV problem with a receiving antenna $M = 32$, parameters $\rho_1 = 1$, $\gamma_1 = 2$, $\eta = 0.0001$ $\rho_2 = 1$, $\gamma_2 = 0.01$, threshold $\in [0, 10]$ for PMD and threshold $\in [0, 5]$ for PFA. Figure 5 compares the estimation accuracy (NMSE) of the two-stage ADMM and MMV-AMP. The impact of signal delay on the estimation accuracy of the MMV-AMP can be very significant, with the estimation accuracy at $T_g = 3$ already worse than the proposed two-stage ADMM at $T_g = 7$. In other words, the proposed two-stage ADMM is superior to the MMV-AMP in terms of estimation accuracy and robustness to signal delay $T_g$. These advantages of the two-stage ADMM are reflected in the fact that the first stage of the algorithm is used to detect whether a user is active in the delay $T_g$. From (25), although the increase in $T_g$ introduces a disturbance in precision, it has less impact on whether the $(\mathbf{E})_i$ is non-zero.

Simulation results of the active user detection performance of the two-stage ADMM are shown in Figs. 6, 7, and 8. Figure 6 gives the effect of the proposed algorithm on detection performance at $Tg = 3$ with different SNRs. From Fig. 6, when the signal delay $T_g$ is fixed, the noise has no significant impact on the PFA but has a greater effect on the PMD. In addition, when the SNRs increase to SNR = 2 dB, the PMD of the algorithm shows a relatively stable trend.

The PMD and PFA performance of the two-stage ADMM algorithm at SNR = 5 dB and for different $T_g$ are

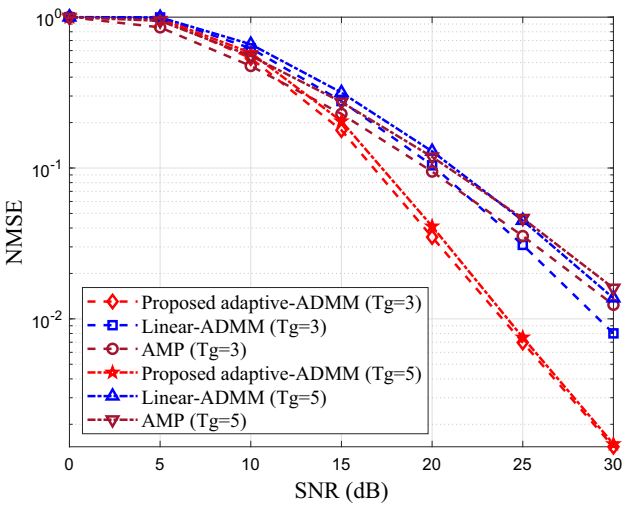


**Fig. 3** NMSE comparison in the SMV problem

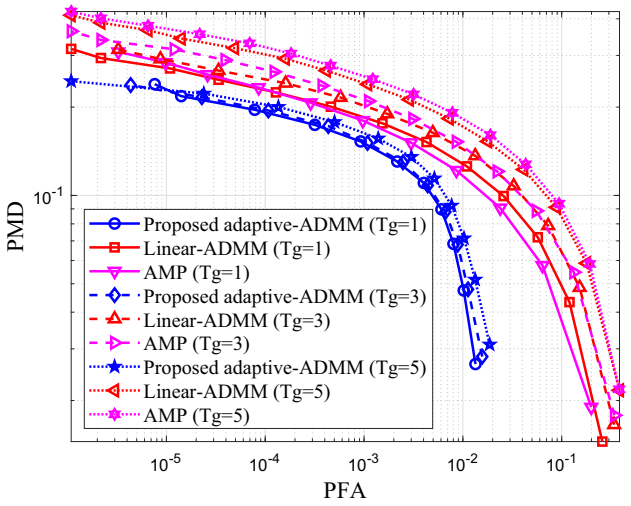


**Fig. 4** Comparison of the algorithm's active user detection performance at SNR = 25 dB

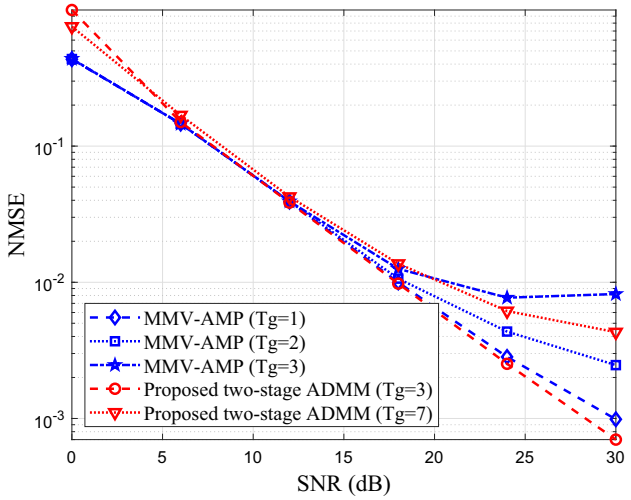


**Fig. 5** NMSE comparison in the MMV problem

given in Figs. 7 and 8, respectively. From the simulation figure, we can see that when the SNRs are constant, the signal delay $T_g$ has a considerable impact on both the PFA and PMD performance of the algorithm. As $T_g$ increases, the PMD gradually decreases while the PFA gradually improves.

Finally, the NMSE of the proposed algorithm for the estimated signals using different initial seeds is given in Table 1. It is assumed that the initial seed used by each user at the transmitter side to generate the pilot is $a_{i,0}$, and the initial seeds used at the receiver side to generate the pilot are $a_{i,0}$, $a_{i,0} + 10^{-6}$ and $a_{i,0} + 10^{-12}(i = 1, 2, ..., N)$. The estimated NMSE shows that the proposed two algorithms have extremely poor estimation performance after slight changes in the initial seeds. Thus, this demonstrates the

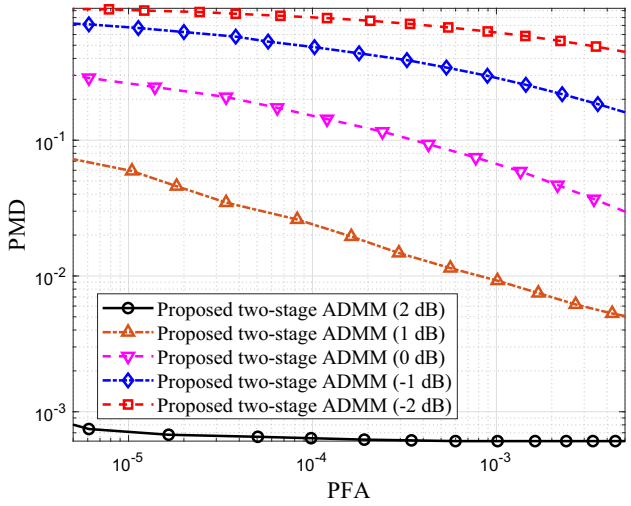


**Fig. 6** Comprehensive performance in the MMV problem for $T_g = 3$

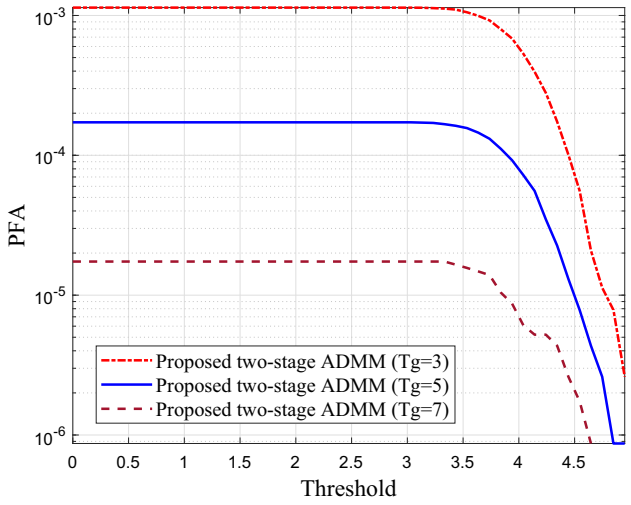


**Fig. 7** PMD of the proposed algorithm at SNR = 5 dB

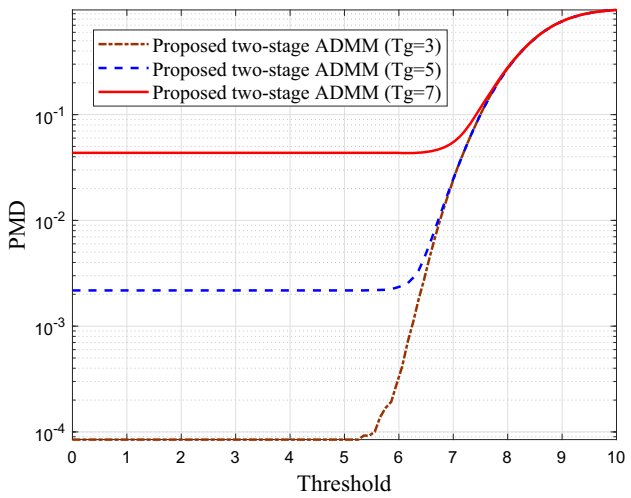


**Fig. 8** PFA of the proposed algorithm at SNR = 5 dB

**Table 1** Comparison of NMSE for estimating with different initial seeds at SNR = 25 dB

| Algorithm | Seeds for recovery | NMSE |
|---|---|---|
| Adaptive-ADMM | $a_{i,0} \quad (i = 1, 2, ..., N)$ | 0.0073 |
| | $a_{i,0} + 10^{-6} \quad (i = 1, 2, ..., N)$ | 0.9995 |
| | $a_{i,0} + 10^{-12} \quad (i = 1, 2, ..., N)$ | 0.9997 |
| Two-stage ADMM | $a_{i,0} \quad (i = 1, 2, ..., N)$ | 0.002 |
| | $a_{i,0} + 10^{-6} \quad (i = 1, 2, ..., N)$ | 1 |
| | $a_{i,0} + 10^{-12} \quad (i = 1, 2, ..., N)$ | 1 |

sensitivity of the estimation performance of the algorithms to the initial seeds.

## 7 Conclusion

This paper proposed two algorithms for joint estimation of activity and channel state information for an asynchronous grant-free NOMA system, which can be applied to massive IoT wireless communications. Due to the high spectral efficiency and low power consumption of the system, it is well suited for underwater acoustic communication, which has higher power requirements. In particular, the pilots generated by chaotic sequences are considered for reducing the pilot storage space. An adaptive ADMM is proposed for the SMV problem, and a two-stage ADMM is proposed for the MMV problem. Simulations show that the proposed two algorithms are computationally efficient while providing superior signal recovery accuracy and activity detection performance. Moreover, the sensitivity of chaotic sequences to initial values is demonstrated. Finally, the proposed algorithm has strong stability for the delay.

**Acknowledgements** Part of this work was presented in ICITES 2022—2th International Conference on intelligent Technology and Embedded Systems. This work of Donghong Cai was supported by the Science and Technology Major Project of Tibetan Autonomous Region of China under Grant No. XZ202201ZD0006G02, the National Natural Science Foundation of China under Grant No. 62001190, the Science and Technology Project of Guangzhou under Grant No. 202201010200, and the China Postdoctoral Science Foundation under Grant No. 2021M691249. The corresponding authors are Donghong Cai and Jing Zhao.

## References

1. Tullberg, H., Popovski, P., Li, Z., Uusitalo, M. A., Hoglund, A., Bulakci, O., Fallgren, M., & Monserrat, J. F. (2016). The METIS 5G system concept: Meeting the 5G requirements. *IEEE Communications Magazine, 54*, 132–139.
2. Abdullah, D. M., & Ameen, S. Y. (2021). Enhanced mobile broadband (EMBB): A review. *Journal of Information Technology and Informatics, 1*, 13–19.
3. Han, M., Duan, J., Khairy, S., & Cai, L. X. (2020). Enabling sustainable underwater IoT networks with energy harvesting: A decentralized reinforcement learning approach. *IEEE Internet of Things Journal, 7*, 9953–9964.
4. Jing, S., Hall, J., Zheng, Y. R., & Xiao, C. (2020). Signal detection for underwater IoT devices with long and sparse channels. *IEEE Internet of Things Journal, 7*, 6664–6675.
5. Liu, Y., Deng, Y., Elkashlan, M., Nallanathan, A., & Karagiannidis, G. K. (2020). Analyzing grant-free access for URLLC service. *IEEE Journal on Selected Areas in Communications, 39*, 741–755.
6. Liu, L., Larsson, E. G., Yu, W., Popovski, P., Stefanovic, C., & De Carvalho, E. (2018). Sparse signal processing for grant-free massive connectivity: A future paradigm for random access protocols in the internet of things. *IEEE Signal Processing Magazine, 35*, 88–99.
7. Vaezi, M., Ding, Z., & Poor, H. V. (2019). *Multiple access techniques for 5G wireless networks and beyond* Vol. 159 (Springer).
8. Liu, Y., Qin, Z., Elkashlan, M., Ding, Z., Nallanathan, A., & Hanzo, L. (2017). Non-orthogonal multiple access for 5G and beyond. *Proceedings of the IEEE, 105*, 2347–2381.
9. Bocus, M. J., Agrafiotis, D., & Doufexi, A. (2018). *Non-orthogonal multiple access (noma) for underwater acoustic communication*, 1–5 (IEEE).
10. Gao, G., Wang, J., Chen, X., Liu, Q., Zhai, R., & Ma, J. (2022). MW-NOMA: An uplink NOMA communication system based on the node pairing algorithm of maximum and minimum weight in underwater acoustic networks. *Wireless Communications and Mobile Computing*. https://doi.org/10.1155/2022/7654456
11. Makled, E. A., & Dobre, O. A. (2022). On the security of full-duplex relay-assisted underwater acoustic network with NOMA. *IEEE Transactions on Vehicular Technology, 71*, 6255–6265.
12. Berger, C. R., Zhou, S., Preisig, J. C., & Willett, P. (2010). Sparse channel estimation for multicarrier underwater acoustic communication: From subspace methods to compressed sensing. *IEEE Transactions on Signal Processing, 58*, 1708–1721.
13. Cai, D., Fan, P., Zou, Q., Xu, Y., Ding, Z., & Liu, Z. (2022). Active device detection and performance analysis of massive non-orthogonal transmissions in cellular internet of things. *Science China Information Sciences, 65*, 1–18.
14. Beltramelli, L., Mahmood, A., Ferrari, P., Österberg, P., Gidlund, M., & Sisinni, E. (2020). Synchronous LoRa communication by exploiting large-area out-of-band synchronization. *IEEE Internet of Things Journal, 8*, 7912–7924.
15. Soatti, G., Savazzi, S., Nicoli, M., Alvarez, M. A., Kianoush, S., Rampa, V., & Spagnolini, U. (2019). Distributed signal processing for dense 5G IoT platforms: Networking, synchronization, interference detection and radio sensing. *Ad Hoc Networks, 89*, 9–21.
16. Ahn, J., Shim, B., & Lee, K. B. (2019). Ep-based joint active user detection and channel estimation for massive machine-type communications. *IEEE Transactions on Communications, 67*, 5178–5189.
17. Donoho, D. L., Maleki, A., & Montanari, A. (2009). Message-passing algorithms for compressed sensing. *Proceedings of the National Academy of Sciences, 106*, 18914–18919.
18. Ziniel, J., & Schniter, P. (2012). Efficient high-dimensional inference in the multiple measurement vector problem. *IEEE Transactions on Signal Processing, 61*, 340–354.
19. Liu, L., & Yu, W. (2018). Massive connectivity with massive MIMO-part I: Device activity detection and channel estimation. *IEEE Transactions on Signal Processing, 66*, 2933–2946.
20. Liu, L., & Yu, W. (2018). Massive connectivity with massive MIMO-part II: Achievable rate characterization. *IEEE Transactions on Signal Processing, 66*, 2947–2959.

21. Kim, J., Chang, W., Jung, B., Baron, D., & Ye, J. C. (2011). Belief propagation for joint sparse recovery. arXiv:1102.3289
22. Chen, Z., Sohrabi, F., & Yu, W. (2018). Sparse activity detection for massive connectivity. *IEEE Transactions on Signal Processing, 66*, 1890–1904.
23. Lin, X., Kuang, L., Ni, Z., Jiang, C., & Wu, S. (2019). Approximate message passing-based detection for asynchronous NOMA. *IEEE Communications Letters, 24*, 534–538.
24. Zhang, R., Wu, X., Li, C., Yan, J., & Zhang, S. (2021). Active user detection and data recovery for quasi-asynchronous grant-free random access (pp. 1–5). IEEE
25. Zhang, X., Ganji, M., & Jafarkhani, H. (2017). Exploiting asynchronous signaling for multiuser cooperative networks with analog network coding (pp. 1–6). IEEE
26. Zou, X., & Jafarkhani, H. (2016). Asynchronous channel training in massive MIMO systems (pp. 1–6). IEEE
27. Kim, S., Kim, J., & Hong, D. (2020). A new non-orthogonal transceiver for asynchronous grant-free transmission systems. *IEEE Transactions on Wireless Communications, 20*, 1889–1902.
28. Jiang, S., Xu, C., Yuan, X., Han, Z., Wang, Z., & Wang, X. (2022). Bayesian receiver design for asynchronous massive connectivity. *IEEE Transactions on Wireless Communications*. https://doi.org/10.1109/TWC.2022.3192927
29. Ding, T., Yuan, X., & Liew, S. C. (2019). Sparsity learning-based multiuser detection in grant-free massive-device multiple access. *IEEE Transactions on Wireless Communications, 18*, 3569–3582.
30. Zhu, W., Tao, M., Yuan, X., & Guan, Y. (2021). Deep-learned approximate message passing for asynchronous massive connectivity. *IEEE Transactions on Wireless Communications, 20*, 5434–5448.
31. Gan, H., Li, Z., Li, J., Wang, X., & Cheng, Z. (2014). Compressive sensing using chaotic sequence based on Chebyshev map. *Nonlinear Dynamics, 78*, 2429–2438.
32. Cirik, A. C., Balasubramanya, N. M., & Lampe, L. (2017). Multi-user detection using ADMM-based compressive sensing for uplink grant-free NOMA. *IEEE Wireless Communications Letters, 7*, 46–49.
33. He, Q., Quek, T. Q., Chen, Z., Zhang, Q., & Li, S. (2018). Compressive channel estimation and multi-user detection in c-ran with low-complexity methods. *IEEE Transactions on Wireless Communications, 17*, 3931–3944.
34. Qiu, M., Cao, K., Cai, D., Dong, Z., & Cui, Y. (2022). Low-complexity joint estimation for asynchronous massive internet of things: An ADMM approach (pp. 13–20). IEEE
35. Wang, Y., & Yin, W. (2010). Sparse signal reconstruction via iterative support detection. *SIAM Journal on Imaging Sciences, 3*, 462–491.
36. Shen, W., Dai, L., Shi, Y., Gao, Z., & Wang, Z. (2016). Massive MIMO channel estimation based on block iterative support detection (pp. 1–6). IEEE
37. Sheta, A. N., Abdulsalam, G. M., & Eladl, A. A. (2021). Online tracking of fault location in distribution systems based on PMUs data and iterative support detection. *International Journal of Electrical Power & Energy Systems, 128*, 106793.
38. Cai, D., Wen, J., Fan, P., Xu, Y., & Yu, L. (2020). Active user and data detection for uplink grant-free NOMA systems. *China Communications, 17*, 12–28.
39. Ganesan, U. K., Björnson, E., & Larsson, E. G. (2021). Clustering-based activity detection algorithms for grant-free random access in cell-free massive MIMO. *IEEE Transactions on Communications, 69*, 7520–7530.




**Mingyi Qiu** received the B.E. degree in Engineering Mechanics from China University of Mining and Technology in 2018. He is currently pursuing a M.E. degree in Cyberspace Security at the School of Information and Technology, Jinan University, Guangzhou. His current research interests include signal processing, Internet of Things.

**Donghong Cai** received the B.S. degree from the School of Mathematics and Information Sciences, Shaoguan University, Shaoguan, China, in 2012, and the M.S. and Ph.D. degrees from Southwest Jiaotong University, Chengdu, China, in 2015 and 2020, respectively. From October 2017 to October 2018, he was a visiting Ph.D. student at Lancaster University and the University of Manchester, UK. He is currently a lecturer with the College of Information Science and Technology/College of Cyber Security, Jinan University, Guangzhou, China. He received the 2nd International Conference on Intelligent Technology and Embedded Systems (ICITES 2022) Best Paper Award and the International Conference on Big Data (ICBD 2023) Best Paper Award. He serves as a Guest Editor for Physical Communication and Electronics. He is the General Chair of the 12th EAI International Conference on Game Theory for Networks (GameNets 2023). His current research interests include signal detection, security coding, distributed Internet of Tings, privacy preservation, semantic communication, and non-orthogonal multiple access.

**Jing Zhao** received the B.S. and Ph.D. degrees in communication engineering and communication and information system from Southwest Jiaotong University, Chengdu, China, respectively. She was a Visiting Ph.D. Student with the Department of Electrical Engineering, University of Arkansas, Fayetteville, USA, from 2014 to 2015. She works in School of Network and Communication Engineering, Chengdu Technological University, Chengdu, China now. Her research interests include the key technology for joint

communication and radio sensing, NOMA, cooperative communications, and signal processing.

**Zhicheng Dong** received the B.E., M.S. and Ph.D. degrees in School of Information Science and Technology from Southwest Jiaotong University, Chengdu, China, in 2004, 2008 and 2016, respectively. From 2013 to 2014, he worked as a visiting scholar in the Department of Electrical and Computer Engineering at Utah State University, USA. From 2018 to 2019, he worked as a research fellow in the Department of Electrical and Computer Engineering at Columbia University, USA. Since 2018, he has been a professor with School of Information Science and Technology, Tibet University, Lhasa, China. He received EAI GameNets 2022 Best Paper Award and 2022 2nd International Conference on Intelligent Technology and Embedded Systems Best Paper Award. He served as track chair and technical sessions chair for 2022 IEEE ICICN. He also served as TPC members for major international conferences such as IEEE ICC, IEEE GLOBECOM, IEEE WCNC, IEEE VTC , IEEE PIMRC, etc. He also served as a reviewer for many well-known journals such as IEEE Wireless Communications Magazine, IEEE Journal on Selected Areas in Communications, IEEE Transactions on CommunicationsIEEE Transactions on Vehicular Technology, etc. His research interests include artificial intelligence, computer vision, adaptation technology, performance analysis and signal processing for high mobility wireless communications.

**Weixi Zhou** received the B.E.degree in communication engineering and the Ph.D. degree in communication and information systems from Southwest Jiaotong University, Chengdu China, in 2009 and 2016, respectively. He was a Visiting Student with the Department of Electrical Engineering, University of Arkansas, Fayetteville, AR, USA in 2014. From 2016 to 2021, he worked at Huawei Technologies Co., Ltd, and he has contributed to 5G communications for both standardization and practical realization. He is a currently a Lecturer in Sichuan Normal University. His research interests include 5G communications, millimeter wave communications, high mobility communications and machine learning techniques.